Deep-Sea Research I 97 (2015) 40–51

Contents lists available at ScienceDirect

Deep-Sea Research I

journal homepage: www.elsevier.com/locate/dsri

Diurnal tides on the Barents Sea continental slope

Jofrid Skarðhamar [a,*], Øystein Skagseth [a,b], Jon Albretsen [a]

[a] Institute of Marine Research (IMR), Postbox 1870 Nordnes, N-5870 Bergen, Norway
[b] Bjerknes Centre for Climate Research, Bergen, Norway

ARTICLE INFO

Article history:
Received 13 January 2014
Received in revised form
21 November 2014
Accepted 25 November 2014
Available online 10 December 2014

Keywords:
Topographic waves
Continental shelf waves
Mesoscale eddies
Shelf slope
Diurnal tides
Numerical modeling
Tromsøflaket
Norway

ABSTRACT

Measurements of diurnal tides over the continental slope between the Norwegian Sea and the Barents Sea shelf are presented. Numerical 3D simulations, in agreement with field data, show strong cross-slope velocities and large vertical displacements of the interface between Atlantic Water and intermediate water over the slope. The striking correspondence between the prominent observed and modeled diurnal oscillations gives confidence that this is well represented by the model. This variability, interpreted as tidally induced diurnal period topographic waves, is confined to the diverging topography of the continental slope west of Tromsøflaket. The model results reveal highly variable magnitudes of the oscillations and the cross shelf currents in time, related to variable strength of the background flow, the Norwegian Atlantic Current. We suggest that the diurnal topographic wave can be an effective mechanism for cross slope exchange between the Norwegian Sea and the Barents Sea shelf, and important for benthic and pelagic biological processes on the shelf and slope.

© 2014 The Authors. Published by Elsevier Ltd. This is an open access article under the CC BY-NC-ND license (http://creativecommons.org/licenses/by-nc-nd/3.0/).

1. Introduction

The ocean circulation in the Nordic Seas is characterized by topographic steering (Helland-Hansen and Nansen, 1909), with the Norwegian Atlantic Current (NAC) carrying warm Atlantic Water (AW) northwards along the Norwegian continental shelf break. Over the continental shelf slope the AW occupies the upper ~600 m of the water column, and below this the colder and less saline intermediate water (IW) is found. Norwegian coastal water (NCW) flows northwards along the coast and over the continental shelf as the Norwegian coastal current (NCC). The vertical and horizontal extent of the NCC varies seasonally, and the front between the NCW and AW is characterized by eddies and meanders (Ikeda et al., 1989; Johannessen et al., 1989). At Tromsøflaket, a bank area at the entrance to the Barents Sea (Fig. 1), the NAC splits into two branches, one flowing eastwards into to the Barents Sea, and the other northwards to Spitsbergen and the Fram Strait (Furevik, 1998, 2001).

There is great interest in understanding the local ocean dynamics and the interaction between the water masses in the Tromsøflaket area to explain the transport mechanisms of plankton (such as fish eggs and *Calanus finmarchicus*) into the Barents Sea (Aksnes and Blindheim, 1996; Edvardsen et al., 2003), the observed distribution of benthic species on the continental shelf and slope (Buhl-Mortensen et al., 2012), and sediment distribution on the seabed (Bøe et al., 2013; King et al., 2014). Previous model studies have shown that the interaction between tides and topography produce topographic waves along the continental slope off Northern Norway (Ommundsen and Gjevik, 2000) and that diurnal components are enhanced at Tromsøflaket (Kowalik and Proshutinsky, 1995). Such waves could initiate large excursions of the interface between AW and intermediate water due to interaction with the sloping bottom. Diurnal topographic waves have been observed both in the Arctic (Hunkins, 1986; Padman et al., 1992), and in the Antarctic (Middleton et al., 1997; Padman et al., 2009). However, observations confirming such variability have so far been lacking for the Northern Norwegian continental margin.

In this paper we present high resolution time series of measured temperature, salinity and currents near the sea bed resolving the diurnal tides on the Tromsøflaket slope. We support the interpretation of these data using simulations with a high-resolution ocean circulation model. We show that the model reproduces the key features of the observations well, and use the model results to discuss the regional differences connected to the bottom slope. In a companion paper (Bøe et al., 2014), these model fields are integrated with geological data to explain the generation and development of sandwaves on the continental slope.

2. Methods

2.1. Numerical modeling

We used an extended version of the 800 m grid model NorKyst800 developed by the Institute of Marine Research (IMR),

* Corresponding author. Tel.: +47 5 523 8500.
E-mail address: jofrid.skardhamar@imr.no (J. Skarðhamar).

http://dx.doi.org/10.1016/j.dsr.2014.11.008
0967-0637/© 2014 The Authors. Published by Elsevier Ltd. This is an open access article under the CC BY-NC-ND license (http://creativecommons.org/licenses/by-nc-nd/3.0/).

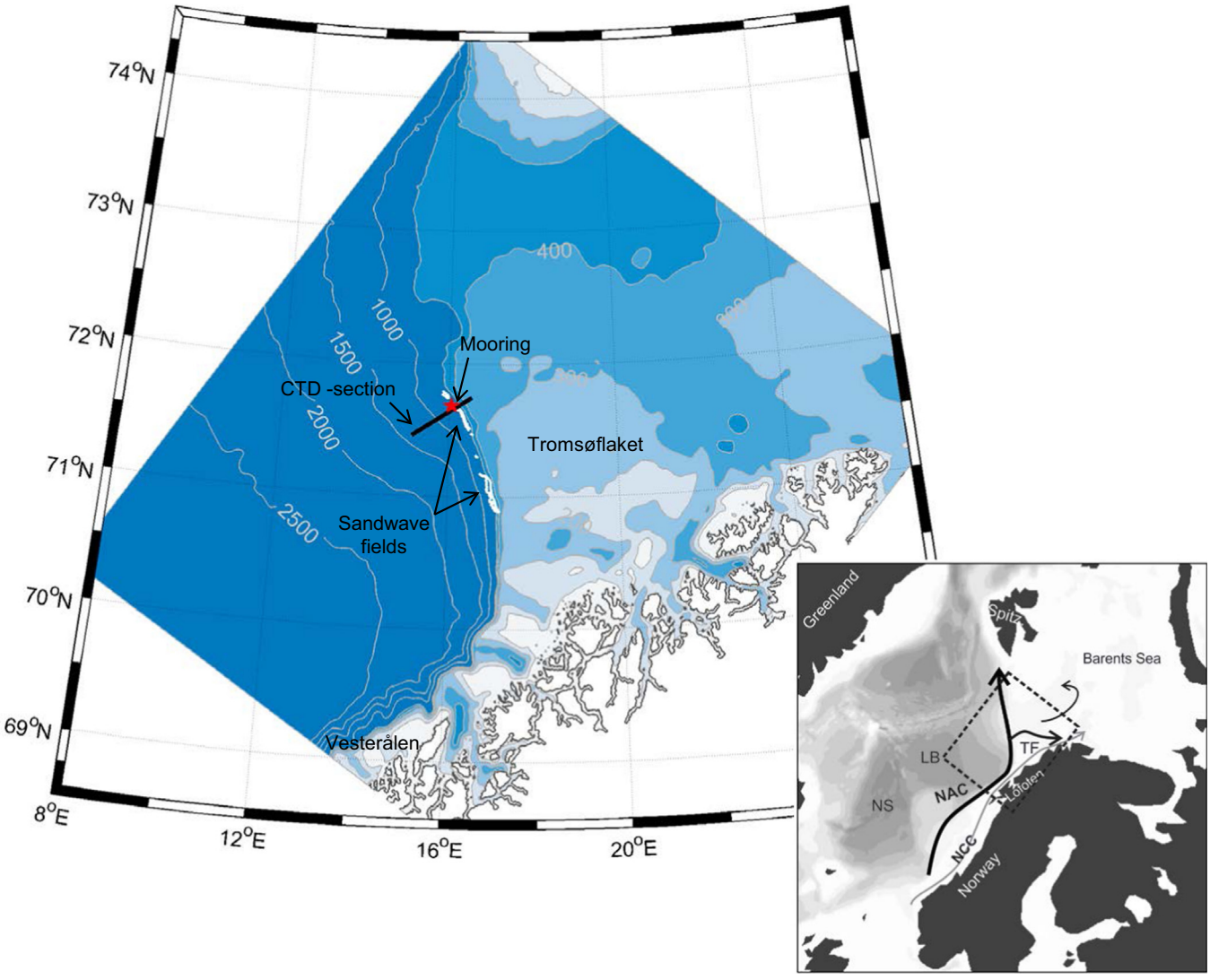

Fig. 1. Bathymetric map of the model domain (left), which is marked with a stipled rectangle in the map of the Nordic Seas (right). NAC: North Atlantic Current, NCC: Norwegian coastal current, NS: Norwegian Basin, LB: Lofoten Basin, TF: Tromsøflaket, Spitz.: Spitsbergen. The red star indicates the position of the current meter mooring, and the black line shows the CTD transect. Isobaths are drawn for depths 100, 200, 300, 400, 500, 1000, 1500, 2000 and 2500 m. The white contours between 70.5 and 72°N marks the positions of the sandwave fields described in Bøe et al. (2014). The coastline is drawn with black contours.

Norwegian Institute for Water Research (NIVA) and Norwegian Meteorological Institute (MET) (Albretsen et al., 2011). NorKyst800 is based on the public domain Regional Ocean Modeling System (ROMS, Haidvogel et al., 2008; Shchepetkin and McWilliams, 2005), which is a 3D free-surface, hydrostatic, primitive equation ocean model using terrain-following *s*-coordinates in the vertical. Our model covered the area shown in

Fig. 1, with 681×611 grid cells in the horizontal, each of size 800 m × 800 m, and 35 terrain-following levels in the vertical. The model was run for 2012 with three months preceding spin up time. Lateral boundary conditions were obtained from the archive of MET's Nordic4km simulation (http://thredds.met.no), and included daily mean currents, salinity and temperature at depths 0, 5, 10, 20, 30, 50, 100, 200, 500 and 1000 m, in addition to surface height. Tidal forcing was based on a global inverse barotropic model of ocean tides (TPXO7.2), including eight primary harmonic constituents (M2, S2, N2, K2, K1, O1, P1, Q1) of semidiurnal and diurnal frequencies, two long period (Mf, Mm) and three nonlinear (M4, MS4, MN4) constituents. River runoff was based on estimated discharge data from the Norwegian Water Resources and Energy Directorate (NVE) (Beldring et al., 2003), and atmospheric forcing from ERA-interim (http://www.ecmwf.int/ research/era/do/get/ era-interim). See Albretsen et al. (2011) for further details about the forcing. The vertical configuration of the model layers and grid resolution were adapted to the original vertical transformation in ROMS and the stretching function by Song and Haidvogel (1994), see Fig. 2. The bottom stress computed in our model application applies a quadratic bottom friction formulation with a drag coefficient equal to 3×10^{-3} and bottom roughness equal to 0. The baroclinic time step used was 1 min, and the barotropic time step was 1 s. Output fields of all variables from the model were saved every hour.

2.2. Field measurements

A current meter mooring was deployed on the slope off Tromsøflaket at depth 630 m in the period 19 March–23 April, 2012 (Fig. 1). The mooring was equipped with one Aanderaa Seaguard current meter and two sensors measuring temperature, salinity and pressure (Seabird Microcat CTD, SBE37). See Table 1 for mooring details and measuring depths. During the recovery cruise 27–30 April, 2012 the shelf and slope were surveyed along a

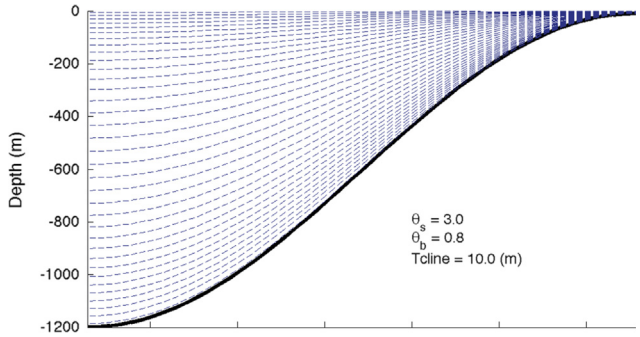

Fig. 2. Vertical layering in the model. The stipled lines show the vertical distribution of the 35 s-levels over a sloping topography, with the given vertical configuration parameters θ_S (*s*-coordinate surface control parameter), θ_b (*s*-coordinate bottom control parameter) and Tcline (with of surface/bottom layer in which higher vertical resolution is required during stretching). See Albretsen et al. (2011) for details of the parametrisation.

Table 1
Current meter mooring 19.03–23.04 2012.

Latitude (°N)	Longitude (°E)	Water depth (m)	Instruments/depth (m above seabed)	Measuring depth above seabed
71.6823	16.0700	632	SBE37 MicroCAT CTD Aanderaa seaguard	60 and 20 m 30 m

Table 2
CTD stations 28–29.04 2012.

St.no	Date	Time (UTC)	Latitude (°N)	Longitude (°E)	Depth (m)
107[a]	28.04 2012	20:25:53	71.7438	16.5347	361
108		21:16:24	71.7028	16.3365	392
109		21:50:32	71.6877	16.2638	496
110		22:28:13	71.6708	16.1798	593
111		23:09:35	71.6540	16.0967	691
112		23:57:26	71.6278	15.9668	792
113	29.04 2012	00:47:04	71.6035	15.8437	893
114		01:43:31	71.5730	15.7117	1009
115		02:59:30	71.5165	15.4382	1205
116		04:29:45	71.4565	15.1330	1400

[a] The salinity data from station 107 were of bad quality, thus salinity and σ_θ from this station were omitted from the data analysis.

cross shelf transect of 10 CTD stations, see Fig. 1 and Table 2 for positions. After the cruise, water samples from the CTD stations were analysed according to IMR's calibration procedure for CTD data. The calibration revealed that the salinity data from one station (no. 107) were of bad quality, thus salinity and derived density data from this station are omitted from further analysis. The original mooring program included three moorings in a triangular array with spacing about 1 km. However, due to trawling fisheries over the slope only the above mentioned mooring was successfully recovered, after being adrift for about four days. The two other moorings were destroyed and adrift a few days after deployment, and therefore provided no data for analysis.

3. Results

3.1. Field measurements

The CTD data from the survey 28–29 April, 2012 show water with salinity >35 in the upper 700 m at all stations (Fig. 3). The

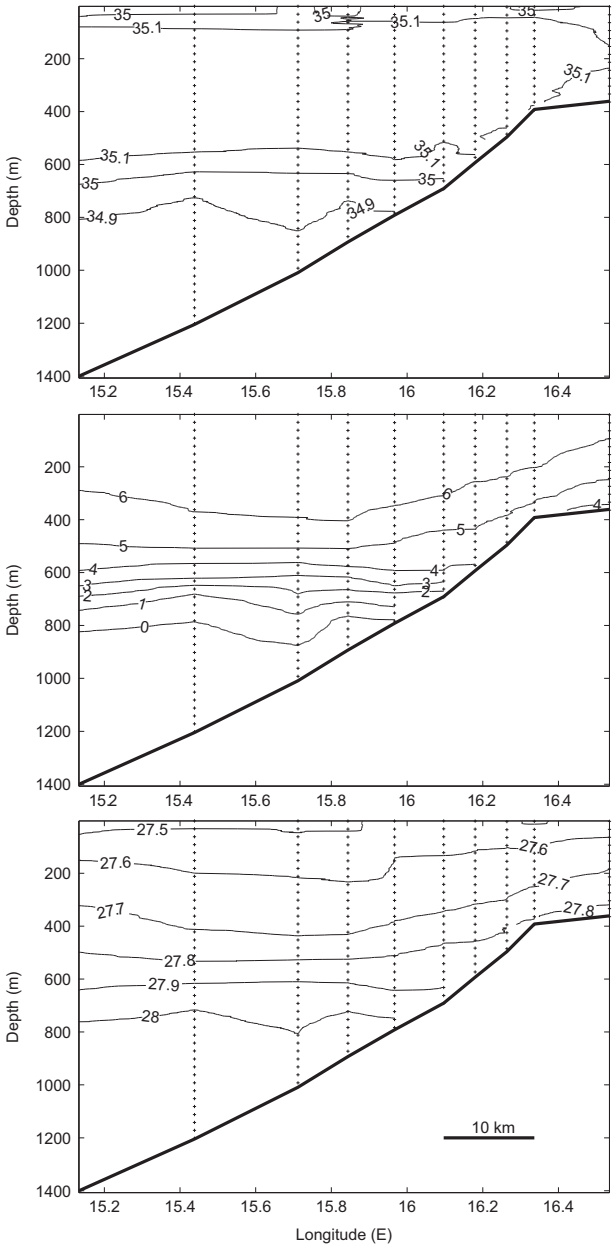

Fig. 3. CTD measurements 28–29 April, 2012. Salinity (upper panel), temperature (°C, mid panel) and density (sigma-theta, lower panel) distribution across the shelf slope west of Tromsøflaket. The dotted vertical lines denote CTD stations, see Fig. 1 and Table 2 for positions.

core of Atlantic Water with salinity >35.1 was found in the depth interval 40–600 m. The temperature decreased with depth, from 6 °C in the upper 400 m to <0 °C below 800 m. At the deepest stations (west of 16°E) the thermocline was pronounced with a temperature change of ~ 5 °C between 500 m and 800 m depth.

Temperature and salinity measurements in the period 19 March–23 April, 2012 from the mooring, are presented in Fig. 4. The temperature fluctuated between 0 °C and 7 °C in the measuring period, with a daily oscillation period at the two measuring depths. The daily mean temperature decreased during the entire measuring period. The salinity followed the temperature oscillations with increasing amplitudes towards the end of the measuring period. The current measurements (Fig. 4, lower panel) were decomposed to cross-slope (defined positive 50° clockwise from north) and along-slope (defined positive 40° anti-clockwise from

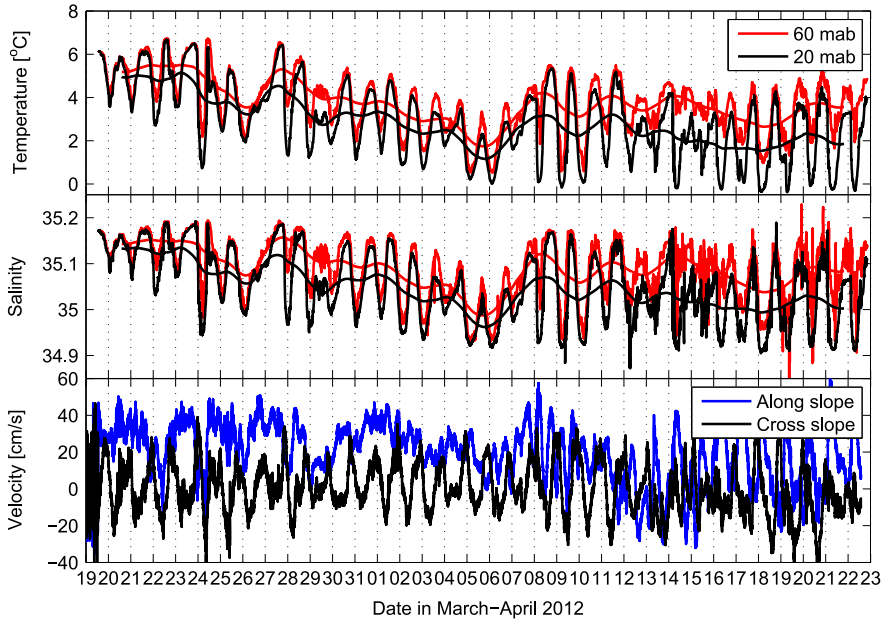

Fig. 4. Time series from 19 March to 22 April, 2012 of measured temperature (upper panel) and salinity (mid panel) from the mooring located on water depth 632 m. Temperature (upper panel) and salinity measurements (mid panel) are from 20 m (black) and 60 m (red) above bottom, i.e. at depth 612 m and 572 m. The smooth lines show the daily mean values. Current measurements (lower panel) are from 30 m above bottom, i.e. 602 m depth: along-slope (blue) and cross-slope (black) current components.

north). The cross slope current velocity component changed daily between ± 0.4 m/s the first ten days, ± 0.25 m/s the first days of April, and ± 0.3–0.4 m/s during mid and end of April, consistent with the expected spring-neap tidal variability with modulation period of ~ 14 days.

3.2. Model evaluation: Model results compared with CTD and mooring data

The modeled salinity and temperature values (Fig. 5) were in the same range as the CTD data (Fig. 3), but the vertical gradients of temperature and salinity were weaker in the model than those measured. However, the modeled density distribution (σ_θ) still agreed with the CTD measurements at the deep stations, where σ_θ increased gradually from 27.5 near the surface to 28.0 at ca. 800 m depth. The modeled Atlantic Water distribution compared well with CTD measurements: AW extends from 50 to 600 m depth, and overlies Intermediate Water of slightly lower salinity (34.92–35.00) and temperature < 2 °C. The intermediate water was more saline and warmer than measured with CTD. The modeled low salinity surface layer of coastal water over the slope was not present in the CTD data. Time series of modeled parameters (Fig. 6) show similar patterns as the mooring data, with daily oscillations in temperature, salinity and cross-slope current velocities. The spring-neap variations are clearly seen for the cross-shelf current component, and also reflected in temperature and salinity in both model and mooring data. As observed, the daily mean temperature and salinity decreased during the period. The modeled temperature, salinity and current velocities were of similar scales as those observed, and also varied with similar periodicity and amplitudes. The measured and modeled distribution of cross- and along-slope current velocity components showed good agreement (Fig. 7), although the model produced a higher proportion of weak along-slope velocities than the measurements. Both model results and mooring data show that the dominant current direction was towards northwest, which is along the slope. However, the modeled current directions were slightly less confined to the slope with a few more events in an off shelf direction than observed (Fig. 8).

3.3. Further model results

The numerical model demonstrates diurnal scale hydrographic variability along the Tromsøflaket slope, where the deep water is moving up and down the slope with a diurnal period. Intermediate water of salinity < 35, temperature < 2 °C and $\sigma_\theta = 28.0$, found in the model below 800 m (Fig. 5), is displaced upwards onto the shelf at 400 m, and down again with a daily periodicity (Fig. 5). Such oscillations were seen in the temperature and salinity time series both from the mooring (Fig. 4) and the model (Fig. 6).

Fourier transformation analysis of the modeled temperature data in the deepest model layer (i.e. close to the seabed) show that tidal variations dominated over the slope. The diurnal signals are strongest in the northern part, while semi-diurnal variability dominates in the southern part of the slope and shelf (Figs. 9 and 10) west of Tromsøflaket. This transition from semi-diurnal to diurnal signal was evident through the whole year, but the extent of the areas with these tidal characteristics varied somewhat between different months (not shown).

Modelled annual time series (Fig. 11) from the mooring position show that the magnitude of the oscillations varies throughout the year, and that cold water (< 1 °C) reached 600 m depth frequently during spring and summer (April–July) and late autumn (November–December) in 2012. The bottom temperature at this location typically varied between 0 °C and 5 °C within the same day. Corresponding modelled time series from 400 m depth show temperatures varying between 0.5 °C and 5 °C in the same periods (not shown). Further to the south, where the slope is steeper, the oscillations are less prominent with only short/single episodes of cold water at 600 m depth (Fig. 11), and never at 400 m depth (not shown).

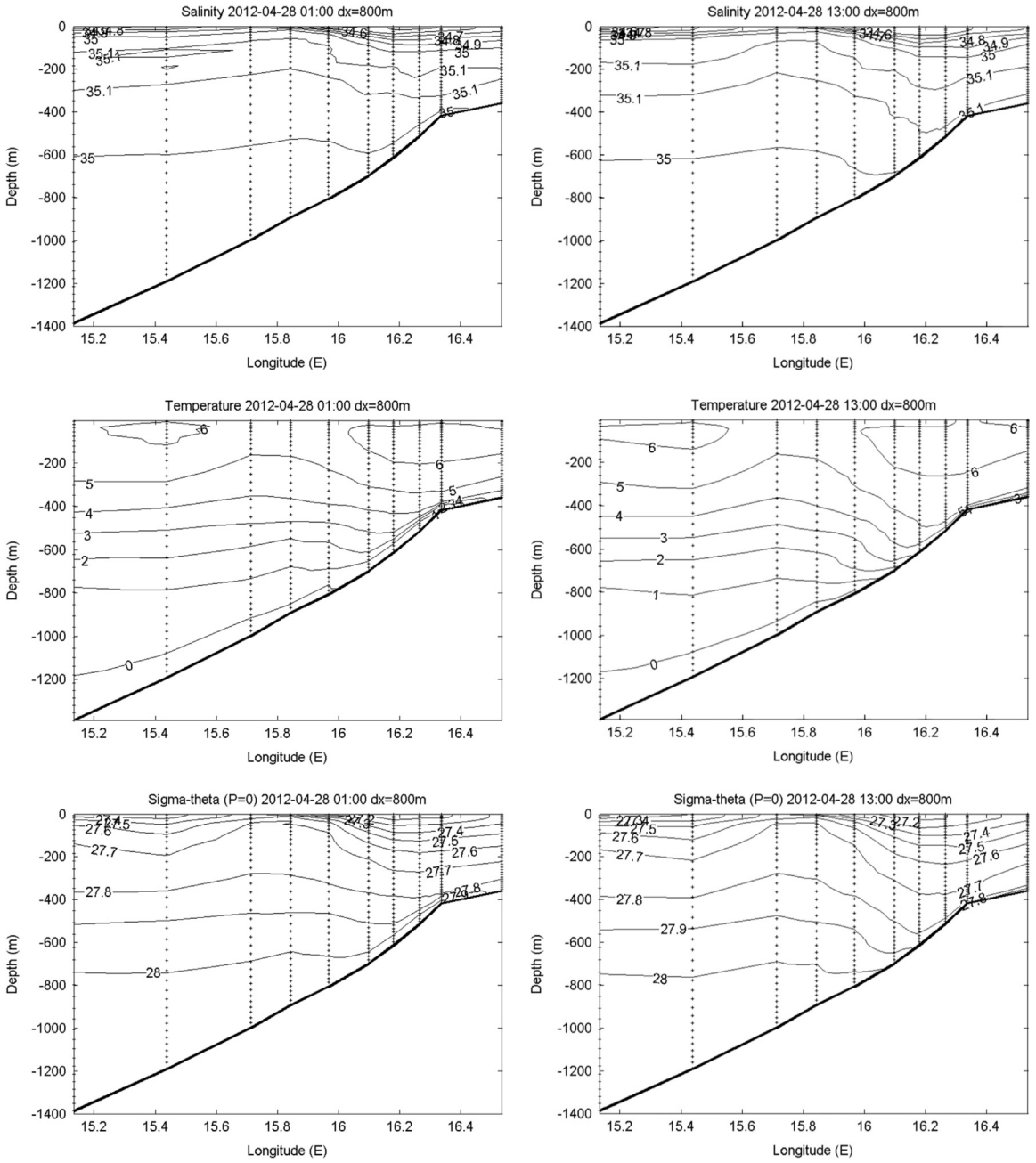

Fig. 5. Modeled salinity, temperature and density (sigma-theta) distribution from the 800 m model setup 28 April, 2012, 03:00 (left panels) and 12 h later, 29 April, 2012, 15:00 (right panels). The section crosses the shelf slope west of Tromsøflaket. The dotted vertical lines denote grid cells representing the CTD stations, see Fig. 1 and Table 2 for positions. Note the isolines moving up and down the slope metween 400 m and 800 m depth.

To investigate the properties of the diurnal signal, the tidal analysis package T_Tide (Pawlowicz et al., 2002) was applied to the current measurements and the modeled velocity series at the mooring site (Fig. 12). The dominant diurnal component (K1) from the current measurements reveal uni-directional variability with the major axis of about 16 cm/s directed in cross slope direction. The modeled current at the same position during the observation period has a comparable dominant uni-directional K1 variability in cross slope direction for the observation period (not shown). However, the major axis current of the K1 component is amplified by a factor of ~3 from its value of ~10 cm/s in January–March to ~29 cm/s in June–August. The barotropic (defined here as the depth-mean) velocity shows a similar amplification, but with lower ellipcity (i.e. larger ratio of the minor/major axes). For both seasons, the depth-averaged K1 current in our model is significantly larger than the value taken from the Padman and Erofeeva (2004) 5 km barotropic inverse tide model.

The modeled current field along the shelf slope is characterized by a northward slope following current, as well as eddies and meanders (Fig. 13). For most of the monthly average current fields there is a pronounced northward flowing current along the slope, with eddies mainly occurring over the deep part of the continental slope. However, for months where the mean slope current is weak, an anti-cyclone is present in the area of the mooring (Fig. 13, April and October). Diurnal alternating anticyclonic and cyclonic vortices appear over the slope at 71°40′N (Fig. 14), which is over one of the sandwave fields in this area (see Fig. 1 and King et al., 2014).

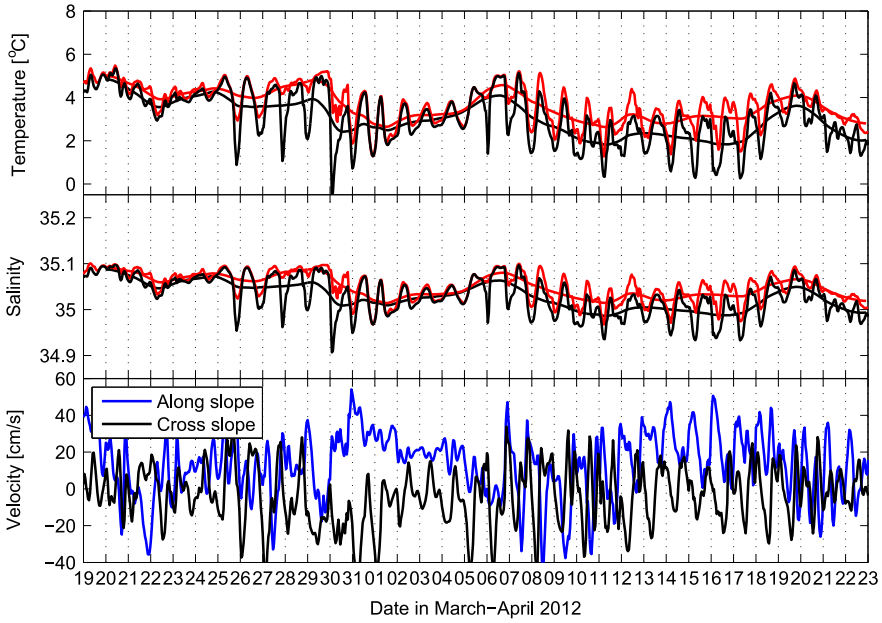

Fig. 6. Modeled time series of temperature (upper panel), salinity (mid panel) and current components across and along the slope (lower panel) in a position representing the mooring, and depths representing the mooring measuring depths (Fig. 4) in the model. The temperature and salinity time series are from model layer depth 608 m (black) and 576 m (red), and the current components are from model layer depth 608 m. The smooth lines show the daily mean values for temperature and salinity.

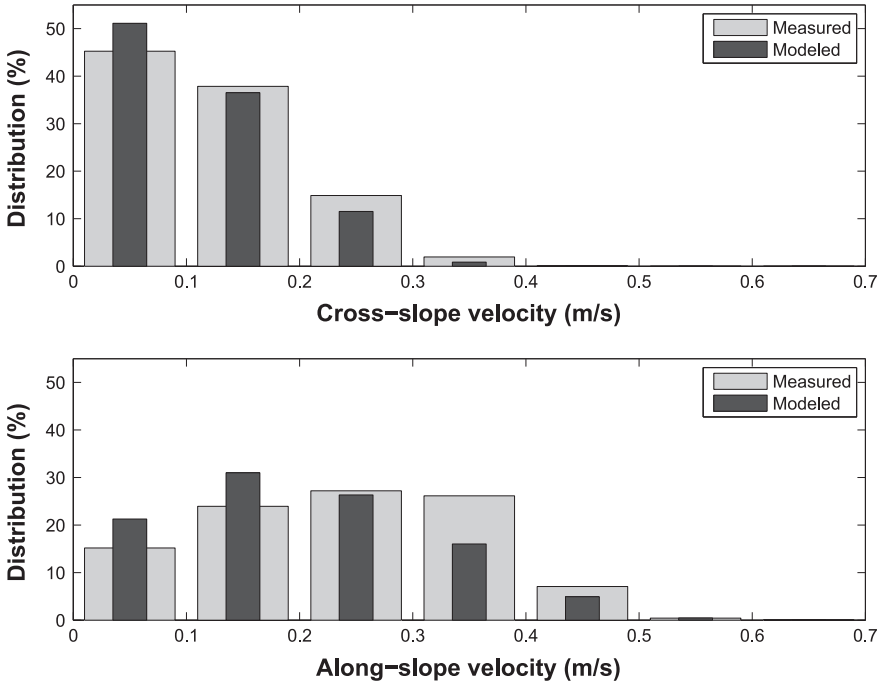

Fig. 7. Distribution of measured and modelled cross-slope and along-slope current velocity components at depth 630 m in the period 18 March–22 April, 2012 at the mooring position.

4. Discussion

The comparison of modeled and measured hydrography and currents shows good agreement. The daily oscillations seen in the mooring data from March to April 2012 are reproduced by the model with respect to range of variability, and there is no clear bias. The modeled depth and properties of the Atlantic Water are similar to observations. There are, however, some discrepancies. The model shows a larger influence of low-salinity coastal water in the surface layer and also a less well-defined interface between the Atlantic Water and the water below. The latter could be due to decreasing vertical resolution of the boundary input fields with depth (below 200 m depth, only input data from 500 m and 1000 m were available). Baroclinic instability and eddy shedding are known to occur at the front between the Coastal water and the Atlantic Water (Johannessen et al., 1989; Mysak and Schott, 1977),

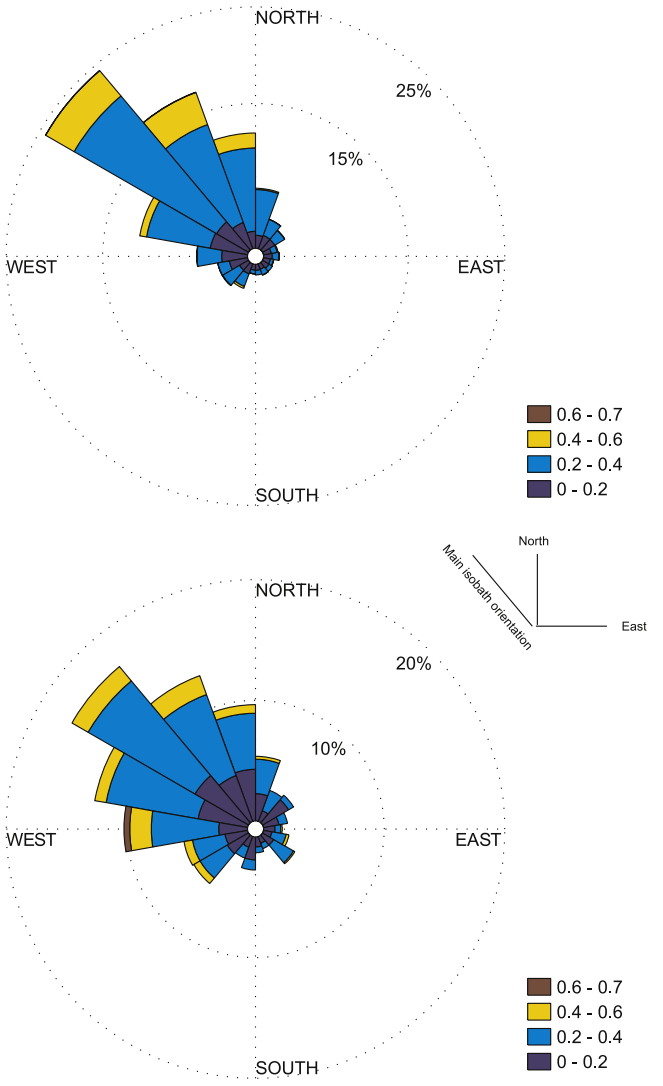

Fig. 8. Measured (upper panel) and modeled (lower panel) distribution of current direction and speed at the Tromsøflaket slope, at position 71°41′N 16°04′E, depth 602–608 m, and period 18 March–22 April, 2012.

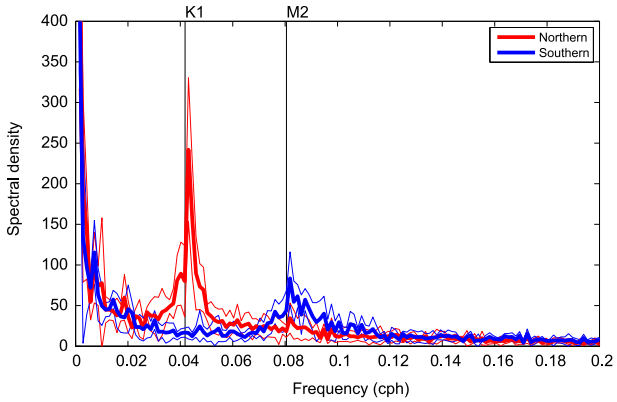

Fig. 9. Fourier transformation (fft) of time series (112 days) of modeled hourly temperature in the deepest model layer at: the mooring position (red) in the Northern sandwave field and one position in the Southern sandwave field (blue), see Fig. 10 for positions. The time series was divided in 5 blocks of 29 days each, and the graphs show the mean signals (thick lines) and standard deviation (thin lines). The frequency of the tidal components M2 and K1 are marked with horizontal lines (K1: 0.0418 cph, M2: 0.0805 cph, Emery and Thomson (2001)).

and meanders and eddies of low-salinity water are periodically present over Tromsøflaket in our model (not shown). In numerical models (non-assimilative) we can expect the *variability* and *extent* of frontal instabilities and eddy shedding to be represented realistically, but not the timing of the occurrence of each eddy and meander. We do not have enough field measurements from the area to evaluate how the model performs for the surface layer (only one transect of CTD stations), but this will be investigated in future projects.

The striking correspondence between the prominent observed and modeled diurnal oscillations at the continental slope gives confidence that this process is well captured by the model. The diurnal signal found in both the observations and in the model appears as a very prominent feature of variability over the continental slope in the western Barents Sea. Such variability has been described by Kowalik and Proshutinsky (1995) who found that the maximum currents in the diurnal band were connected to topographic shelf waves. There have been several other model studies of diurnal tides in the Arctic (Gjevik et al., 1994; Gjevik and Straume, 1989; Hunkins, 1986; Kowalik and Proshutinsky, 1993; Padman and Erofeeva, 2004), but these have been performed with 2D and/or purely tidal models. The present work shows for the first time measurements of and modeled diurnal tides at Tromsøflaket. Our model simulations were carried out in 3D with realistic forcing (winds, tides, freshwater and background flow through the model boundaries) and water mass stratification, which is necessary for obtaining the temporal variability seen in diurnal tidal energy. The tidal forcing of these waves is also supported by current meter data from the fall of 2010, clearly indicating a barotropic signal and spring/neap modulation of the tidal amplitudes (Bøe et al., 2014). Lagrangian float experiments and satellite altimetry have revealed a large-scale quasi-stationary anticyclonic eddy (Gascard and Mork, 2008), and in previous 3D model results of Skarðhamar and Svendsen (2005), a vortex with K1 amplification appeared in the same region where we here find diurnal signals. Padman et al. (1992) interpreted amplification of the diurnal signal at the continental slope of the Yermak Plateau (North-West of Svalbard) as propagating barotropic shelf waves. The mechanism was discussed by Thomson and Crawford (1982) who suggested that the energy input at a location where the group velocity is near zero will allow maximum amplification, but with some topographic leakage, possibly in both directions, along the slope. The continental shelf slope west of Northern Norway is steepest outside Vesterålen, where the inclination of the slope is approximately 4.2°. Further North the slope turns and broadens (Fig. 1), and west of Tromsøflaket the inclination decreases gradually to about 2.6° at the southern sandwave field (see Fig. 1 for locations) and about 1.3° in the area of our mooring position in the northern sandwave field (Bøe et al., 2014; King et al., 2014). Our modeling results show larger vertical amplitudes (~ 400 m) in the northern part of the slope (mooring position) than further south (Figs. 5 and 11). The model results also show stronger diurnal signals during the summer months (Jun–Aug) with a relatively weak slope current compared to the winter months (Jan–Mar).

These results can be compared with the dispersion relation for continental shelf waves (CSW) obtained running the model for CSWs described by Brink (2006) with reasonable sets of input parameters (Fig. 15). The general results of the sensitivity runs are in agreement with Jensen et al. (2013). That is, for a given wavelength, the frequency of CSW increases with both decreasing cross-shelf scale (steeper) and with increasing stratification. The effect of increasing the background flow (the NAC) is to decrease the frequency. When run with a realistic

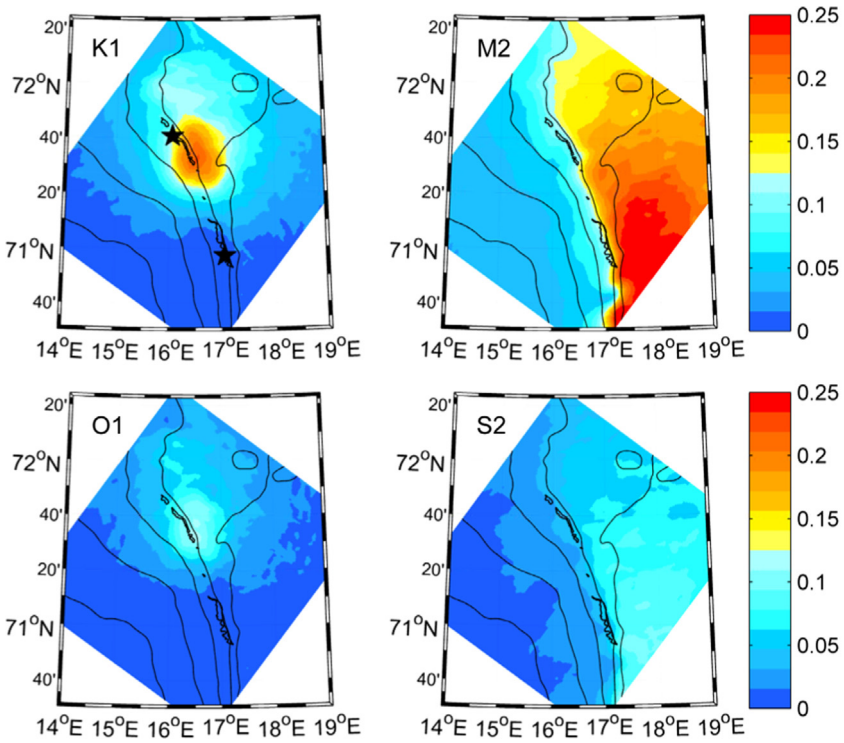

Fig. 10. Magnitudes of the major axis of the tidal components K1, M2, O1, S2, computed with t_tide (Pawlowicz et al., 2002) from the modelled barotropic velocities in each model grid cell, April 2012. Depth contours (black lines) are drawn for depths 300, 500, 1000, 1500 and 2000 m. The black closed contours mark the sandwave fields. The stars in the upper left panel mark positions for the time series in Figs. 10 and 11.

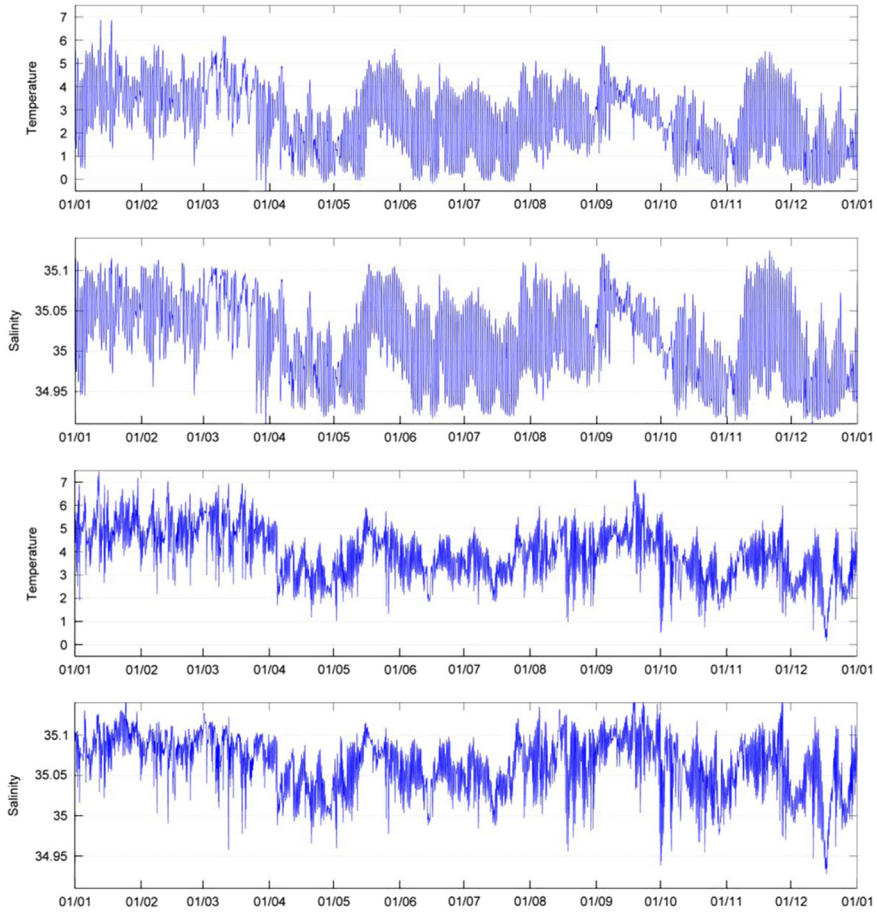

Fig. 11. Time series of modelled bottom temperature and salinity on 600 m depth at 71°40′N, at the mooring position (upper two panels) and further south along the slope at 71°N (lower panels), simulated with the NorKyst800 model for 2012. See Fig. 9 for positions.

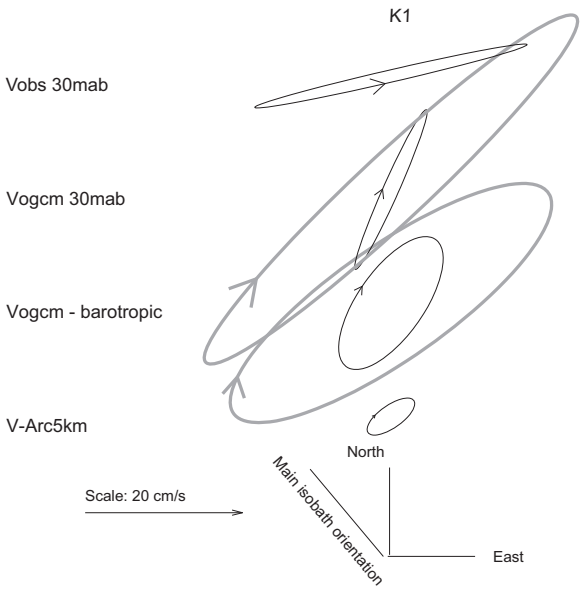

Fig. 12. Tidal ellipses for the K1 component based on the measured current Mar–Apr 2012 30 m above the seabed (upper panel, Vobs), the modeled current (second upper panel, V-ogcm) at the position and depth of the measurements for the period Jan–Mar 2012 (thin black line) and Jun–Aug 2012 (thick grey), the modeled depth mean current (second lower panel, Vogcm—barotropic) at the position of the measurements for the period Jan–Mar 2012 (thin black) and Jun–Aug 2012 (thick grey), and (lower panel, V-Arc5 km) the tidal velocity based on the Arctic 5 km barotropic tidal model (Padman and Erofeeva, 2004). The tidal analysis was performed using the T-Tide Matlab package of Pawlowicz (Pawlowicz et al., 2002). The main isobaths direction is indicated in the figure, and a reference vector of 20 cm/s indicates the magnitude of the ellipses.

topography and stratification for the northern sandwave area (near the mooring position) the dispersion curve intercepts the diurnal period at wavelengths of ~500 km and with zero group velocity (see Fig. 15). In the case of a weak background flow this could lead to non-propagating energy of CSWs. The dispersion curves for the steeper topography further south intercepts the diurnal period at wavelength ~1000 km, but due to large positive group velocities the energy will propagate rapidly out of the area. There is also an intercept at ~150 km and group velocity ~ −40 cm/s for the case of a 25 cm/s mean flow. The dispersion curves obtained taking the mean of the northern and southern topography intercepts the diurnal band at wavelengths of 150 km for the case of a 25 cm/s background flow. The intercept for the weaker background flow is at wavelengths ~100 km and negligible group velocity. These idealized runs indicate that somewhere along the diverging slope, stratification and the strength of the NAC allows wavenumber–frequency pairs at the diurnal period and weak group velocity that balance the slope current. Here the energy may leak away (slowly) in both directions. On a diverging slope, energy going one way can "speed up"; energy going the other way might reach a point where it cannot propagate any more. This is in accordance with Kowalik and Proshutinsky (1995) who noted that diurnal period continental shelf waves were found in the proximity of strong divergence in the bathymetric field. The effect of stratification is to increase the frequency for a given wavenumber thus giving southward group velocities in the range 0–20 cm/s that could balance the mean northward current. These dispersion curves are idealized without along slope bathymetric changes, and the results point to the importance of having realistic 3D currents in

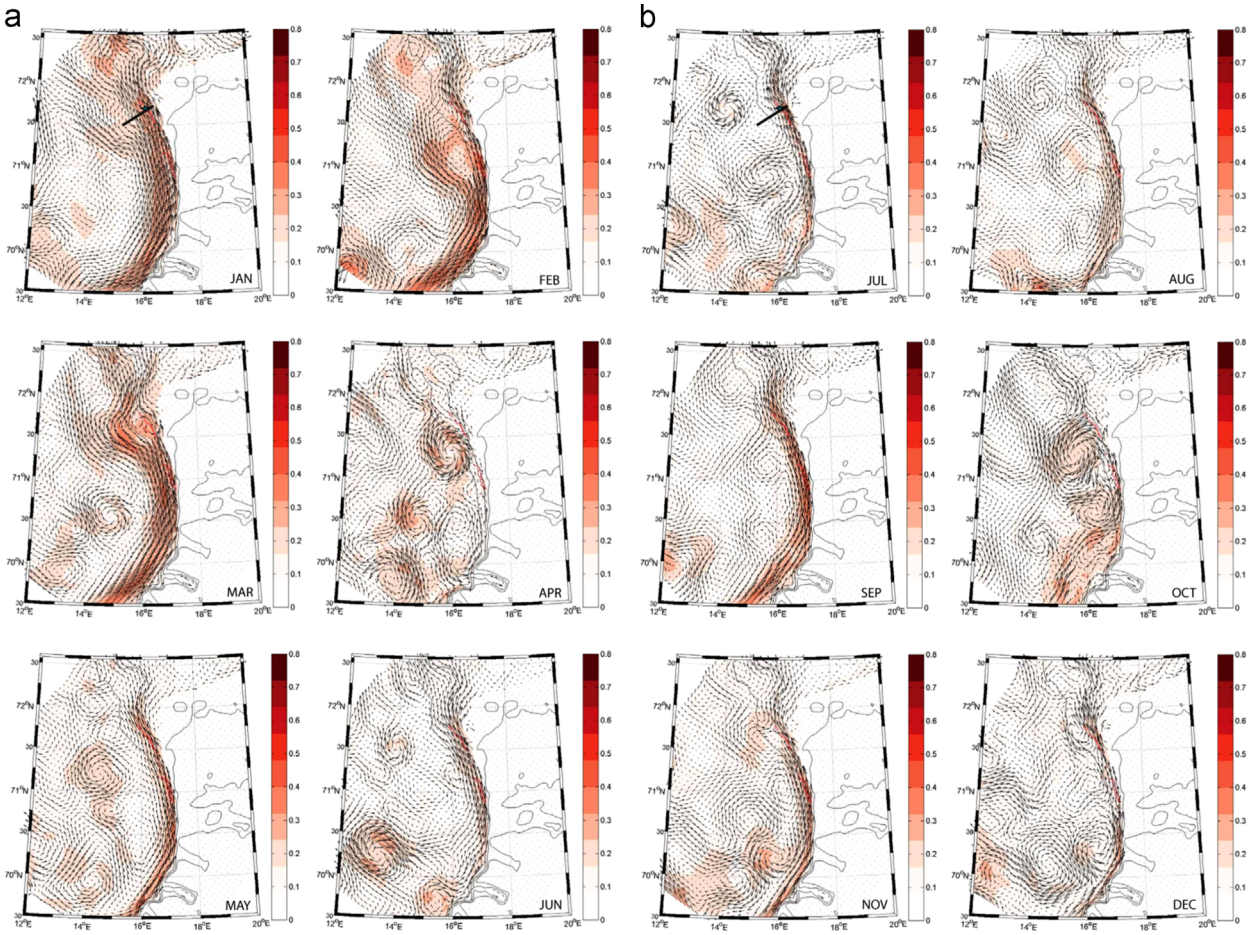

Fig. 13. Modeled monthly mean current speed (colour scale, m/s) and velocity vectors January–December 2012 for depth 350 m. Bathymetric contours for depths 200, 300, 500 and 1000 m are indicated with black lines. For reference, the CTD transect and the position of the current meter mooring is marked with a thick black line and a blue dot in the upper left panels on each page (January and July).

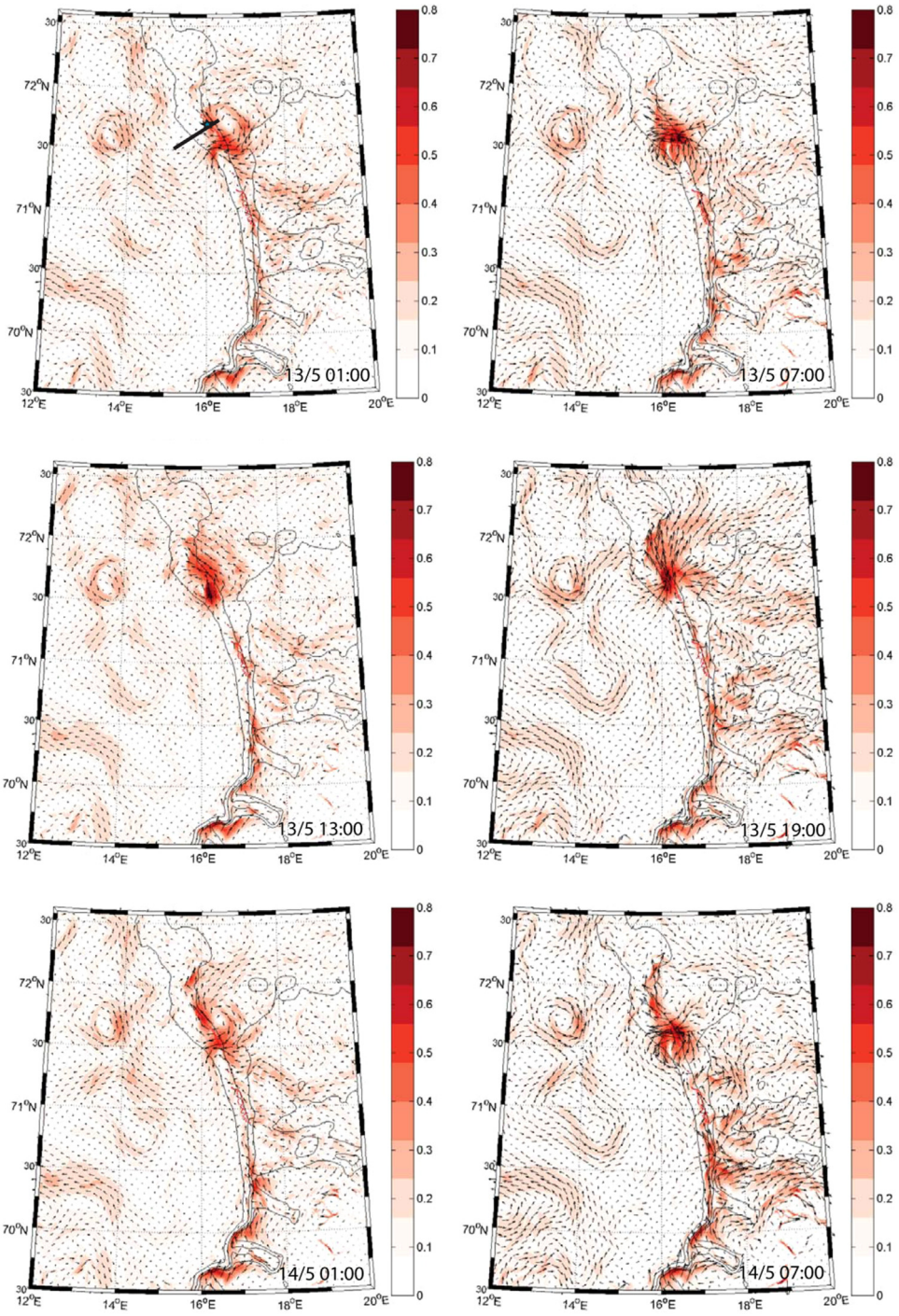

Fig. 14. Modeled bottom current speed (m/s) and velocity vectors from mid May. Bathymetric contours for depths 200, 300, 500 and 1000 m are indicated with black lines. For reference, the CTD transect and the position of the current meter mooring is marked with a thick black line and a blue dot in the upper left panel. Note the anticyclone appearing at 71°45′N, 16°20′E around midnight every day.

ocean models for studies of tidal amplification at diurnal frequencies.

The effect of the baroclinicity of the topographic waves can be neglected in the case of Burger number, $S=(N/f)\ dh/dy<0.2$, where N is the buoyancy frequency, f is the Coriolis parameter, and dh/dy is an estimate of the bottom slope (Chapman and Hendershott, 1982). In the core region of the continental shelf waves, at about 600 m depth, the approximate values of $N=0.002\ s^{-1}$, $f=1.2\times10^{-4}\ s^{-1}$, and the bottom slope $dh/dy=0.02$ give $S=0.33$. This suggests that baroclinicity may play a role, but profiling current meter records from the same region showed only negligible velocity shear (Bøe et al., 2014) supporting the applicability of the barotropic assumption of these topographic waves. The large diurnal period cross-slope velocities lead to large perturbations of the density interface between the warm Atlantic and the colder water beneath. Free internal wave packets at frequencies higher than the fundamental diurnal tide may develop in the pycnocline, and Padman and Dillon (1991) have shown that the dissipation rate at the pycnocline has a strong diurnal component of variability at the Yermak Plateau.

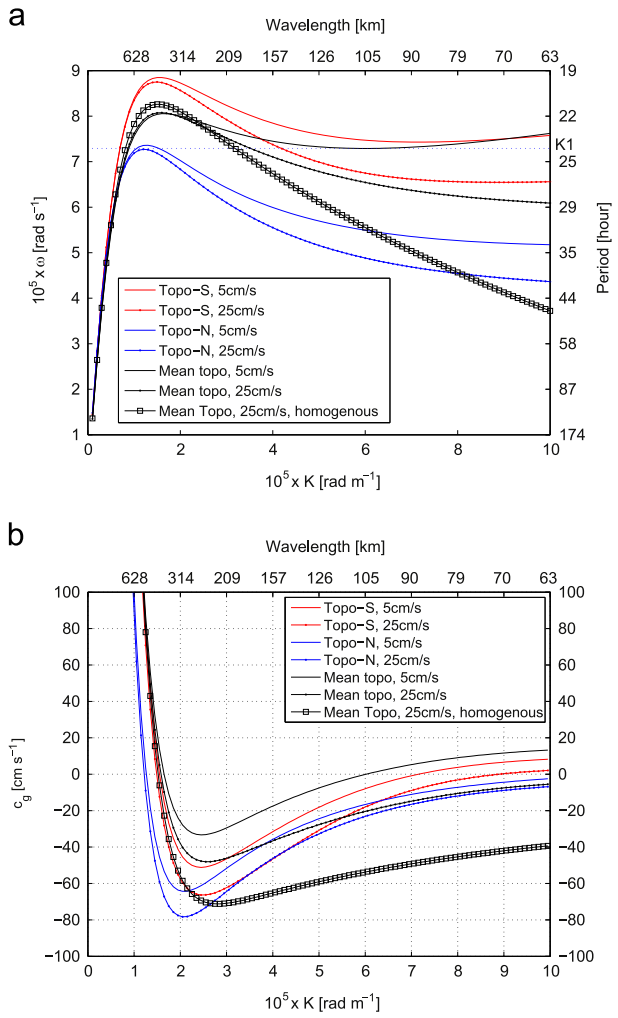

Fig. 15. The modeled (a) dispersion relation (b) and group velocities for different topography (slopes), along-slope velocities and stratification using the Brink (2006) model. Topo-S is at 70.5°N (directed east–west normal to the slope), Topo-N is at 71.5°N (oriented northeast to southwest), Mean topo is the average of Topo-S and Topo-N. The current is centered at the shelf break with an *e*-folding distance of 10 km in both inshore and offshore directions, the stratification is for spring 2012 (Fig. 3). For case "homogeneous" the stratification parameter is $N^2 \times 0.1$. The topography is taken from ETOPO-5.

In a study of the Weddell Sea, temporal variability at the 35 h period was interpreted as coastally trapped waves with group velocity in the opposite direction of a low-frequency varying background current (Jensen et al., 2013). Our results can be interpreted in a similar manner, such that when considering resonant topographic waves at the continental slope the background current, the NAC, is not constant and accordingly, the dispersion of wave energy along the continental slope will vary. During months with a strong NAC (Jan–Mar) there is relatively little sign of eddies as the energy is dissipated northward in the main current direction. In comparison, in Jun–Aug the weaker northward flow of the NAC could be nearly opposed by the group velocity of the continental shelf waves at the diurnal frequency (K1) hence leading to an amplified diurnal variability (Figs. 12 and 13).

An important issue related to topographic shelf waves is the transport of particles (sediments or biota) across the slope. With the cross slope velocity varying as $u = \mathrm{a.cos}(2\pi\omega/T)$, where a is the amplitude, and ω is the angular frequency and T is the period of K1, the cross-slope length scale is $dx = aT/\pi$. A typical cross-slope amplitude of 20 cm/s gives a horizontal displacement of 5.5 km, and a vertical displacement at the bottom of 125 m. The modeled amplitudes of about 200 m may be in the higher end, but a realistic vertical displacement. We suggest that the topographic waves along Tromsøflaket regularly bring cold deep water onto the shelf in specific regions of the slope and thus may affect the distribution of benthic species in the area. These waves can also contribute to increased cross slope supply of nutrients from deep waters onto the shelf, thus supporting increased primary production. Zooplankton migration from deep waters (> 800 m) towards the surface in spring may also benefit from upward transport by topographic waves.

5. Conclusions

Observations from March to April 2012 that quantify the diurnal tide at the continental slope connecting the Barents Sea and the Norwegian Sea are presented. The current ellipse for the diurnal tidal harmonic K1 is almost linear, with a cross-slope component of ~16 cm/s. Extending these results using a high resolution ocean model, we interpret this variability as continental shelf waves. Our results suggest that there is a location along the continental slope where the combined effects of topography, stratification and mean flow lead to conditions favourable to excitation of diurnal continental shelf waves by the large-scale background tide. Also based on the model we find a marked low-frequency variability in the amplitude of the diurnal variability connected to the strength of the background flow, the Norwegian Atlantic Current. Both the measurements and the model results show daily oscillations in temperature, salinity and cross-slope current velocities, coinciding with modeled diurnal displacements of the pycnocline, between Atlantic Water and Intermediate Water, from approximately 800 m on the slope to the shelf break at 400 m depth. In general this cross-slope diurnal variability may be of importance for cross-slope fluxes of physical and biological properties, and this exchange could be the strongest during summer.

Acknowledgement

This research was supported by the Norwegian Deepwater Programme (NDP), and was conducted in collaboration with The Geological Survey of Norway (NGU) through the project "Sandwaves and sand transport on the Barents Sea continental margin". We thank the captain and crew on RV Johan Hjort for cooperation on two cruises, Erik Berg for sharing cruise time with us for deployment of moorings, and the Norwegian coast guard who recovered one of our moorings adrift in sea. The Matlab code to calculate the dispersion curves in Fig. 15 were kindly provided by K.H. Brink. We thank Laurie Padman and one anonymous reviewer for helpful comments on the manuscript.

References

Aksnes, D.L., Blindheim, J., 1996. Circulation patterns in the North Atlantic and possible impact on population dynamics of *Calanus finmarchicus*. Ophelia 44 (1-3), 7–28.

Albretsen, J., Sperrevik, A.K., Staalstrøm, A., Sandvik, A.D., Vikebø, F., Asplin, L., 2011. NorKyst-800 Report no. 1: User Manual and Technical Descriptions. Fisken og havet 2, Havforskningsintituttets Rapportserie, Institute of Marine Research.

Beldring, S., Engeland, K., Roald, L.A., Sælthun, N.R., Voksø, A., 2003. Estimation of parameters in a distributed precipitation-runoff model for Norway. Hydrol. Earth Syst. Sci. 7, 304–316.

Brink, K.H., 2006. Coastal-trapped waves with finite bottom friction. Dyn. Atmos. Oceans 41, 172–190.

Buhl-Mortensen, L., Buhl-Mortensen, P., Dolan, M.F.J., Dannheim, J., Bellec, V., Holte, B., 2012. Habitat complexity and bottom fauna composition at different scales

on the continental shelf and slope of northern Norway. Hydrobiologia 685, 191–219.
Bøe, R., Skarðhamar, J., Rise, L., Dolan, M., Bellec, V., Winsborrow, M., Skagseth, Ø., Knies, J., King, E.K., Walderhaug, O., Chand, S., Buenz, S., Mienert, J., 2014. Sandwaves and Sand Transport on the Barents Sea Continental Margin Offshore Northern Norway. Submitted 2013.
Bøe, R., Winsborrow, M., Rise, L., Dolan, M., Chand, S., Knies, J., Walderhaug, O., Bellec, V., 2013. Sandwaves and Sand Transport on the Barents Sea Continental Margin, Report no. 2013.005., Geological Survey of Norway, Trondheim, 85 pages.
Chapman, D.C., Hendershott, M.C., 1982. Shelf wave dispersion in a geophysical ocean. Dyn. Atmos. Oceans 7 (1), 17–31.
Edvardsen, A., Slagstad, D., Tande, K.S., Jaccard, P., 2003. Assessing zooplankton advection in the Barents Sea using underway measurements and modelling. Fish. Oceanogr. 12 (2), 61–74.
Emery, W.J., Thomson, R.E., 2001. Data analysis Methods in Physical Oceanography. Elsevier Science B.V, Amsterdam, The Netherlands.
Furevik, T., 1998. On the Atlantic Inflow in the Nordic Seas: Bifurcation and Variability. Dr. Scient. Thesis. University of Bergen, Bergen.
Furevik, T., 2001. Annual and interannual variability of Atlantic Water temperatures in the Norwegian and Barents Seas: 1980–1996. Deep Sea Res. Part I 48 (2), 383–404.
Gascard, J.C., Mork, K.A., 2008. Climatic importance of large scale and mesoscale circulation in the Lofoten Basin deduced from lagrangian observations during ASOF. In: Dickson, B., Meincke, J., Rhines, P. (Eds.), Arctic—Subarctic Ocean Fluxes: Defining the Role of the Northern Seas in Climate. Springer Verlag, Nederland.
Gjevik, B., Nost, E., Straume, T., 1994. Model simulations of the tides in the Barents Sea. J. Geophys. Res. Oceans 99 (C2), 3337–3350.
Gjevik, B., Straume, T., 1989. Model simulations of the M_2 and K_1 tide in the Nordic Seas and the Arctic Ocean. Tellus 41A, 73–96.
Haidvogel, D.B., Arango, H., Budgell, W.P., Cornuelle, B.D., Curchitser, E., Di Lorenzo, E., Fennel, K., Geyer, W.R., Hermann, A.J., Lanerolle, L., Levin, J., McWilliams, J.C., Miller, A.J., Moore, A.M., Powell, T.M., Shchepetkin, A.F., Sherwood, C.R., Signell, R.P., Warner, J.C., Wilkin, J., 2008. Ocean forecasting in terrain-following coordinates: formulation and skill assessment of the Regional Ocean Modeling System. J. Comput. Phys. 227 (7), 3595–3624.
Helland-Hansen, B., Nansen, F., 1909. The Norwegian Sea: Its Physical Oceanography Based Upon Norwegian Researches 1900–1904. Det Mallingske bogtrykkeri, Kristiania.
Hunkins, K., 1986. Anomalous diurnal tidal currents on the Yermak Plateau. J. Mar. Res. 44 (1), 51–69.
Ikeda, M., Johannessen, J.A., Lygre, K., Sandven, S., 1989. A process study of mesoscale meanders and eddies in the Norwegian coastal current. J. Phys. Oceanogr. 19, 20–35.
Jensen, M., Fer, I., Darelius, E., 2013. Low frequency variability on the continental slope of the southern Weddell Sea. J. Geophys. Res. Oceans 118 (9), 4256–4272.
Johannessen, J.A., Svendsen, E., Sandven, S., Johannessen, O.M., Lygre, K., 1989. Three-dimensional structure of mesoscale eddies in the Norwegian coastal current. J. Phys. Oceanogr. 19 (1), 3–19.
King, E.K., Bøe, R., Bellec, V., Rise, L., Skarðhamar, J., Ferre, B., Dolan, M., 2014. Contour current driven continental slope-situated sandwaves with effects from secondary current processes on the Barents Sea margin offshore Norway. Mar. Geol. 353, 108–127.
Kowalik, Z., Proshutinsky, A.Y., 1993. Diurnal tides in the Arctic-Ocean. J. Geophys. Res. Oceans 98 (C9), 16449–16468.
Kowalik, Z., Proshutinsky, A.Y., 1995. Topographic enhancement of tidal motion in the western Barents Sea. J. Geophys. Res. Oceans 100 (C2), 2613–2637.
Middleton, J.H., Foster, T.D., Foldvik, A., 1997. Diurnal shelf waves in the Southern Weddell Sea. J. Phys. Oceanogr. 17, 784–791.
Mysak, L., Schott, F., 1977. Evidence of baroclinic instability in the Norwegian Current. J. Geophys. Res. 82 (15), 2087–2095.
Ommundsen, A., Gjevik, B., 2000. Scattering of Tidal Kelvin Waves Along Shelves Witch Vary in Their Lengthwise Direction. Preprint Series, Mechanics and Applied Mathematics. University of Oslo. ⟨https://www.duo.uio.no/handle/10852/10279⟩.
Padman, L., Dillon, T.M., 1991. Turbulent mixing near the Yermak Plateu during the coordinated eastern Arctic experiment. J. Geophys. Res. 96, 4769–4782.
Padman, L., Erofeeva, S., 2004. A barotropic inverse tidal model for the Arctic Ocean. Geophys. Res. Lett. 31 (2), 4.
Padman, L., Howard, S.L., Orsi, A.H., Muench, R.D., 2009. Tides of the northwestern Ross Sea and their impact on dense outflows of Antarctic Bottom Water. Deep Sea Res. Part II 56 (13-14), 818–834.
Padman, L., Plueddemann, A.J., Muench, R.D., Pinkel, R., 1992. Diurnal tides near the Yermak plateau. J. Geophys. Res. Oceans 97 (C8), 12639–12652.
Pawlowicz, R., Beardsley, R., Lentz, S., 2002. Classical tidal harmonic analysis including error estimates in MATLAB using T-TIDE. Comput. Geosci. 28, 929–937.
Shchepetkin, A.F., McWilliams, J.C., 2005. The regional oceanic modeling system (ROMS): a split-explicit, free-surface, topography-following-coordinate oceanic model. Ocean Modell. 9 (4), 347–404.
Skarðhamar, J., Svendsen, H., 2005. Circulation and shelf-ocean interaction off North Norway. Cont. Shelf Res. 25 (12-13), 1541–1560.
Song, Y., Haidvogel, D.B., 1994. A semi-implicit ocean circulation model using a generalized topography-following coordinate system. J. Comp. Phys. 115 (1), 228–244.
Thomson, R.E., Crawford, W.R., 1982. The generation of diurnal period shelf waves by tidal currents. J. Phys. Oceanogr. 12 (7), 635–643.